Eur. Phys. J. C 21, 631–647 (2001)
Digital Object Identifier (DOI) 10.1007/s100520100757

THE EUROPEAN PHYSICAL JOURNAL C

The Lund fragmentation process for a multi-gluon string according to the area law

B. Andersson[a], S. Mohanty[b], F. Söderberg[c]

The Department of Theoretical Physics, Lund University, Sölvegatan 14A, 22362 Lund, Sweden

Received: 3 July 2001 /
Published online: 31 August 2001 –

Abstract. The Lund area law describes the probability for the production of a set of colourless hadrons from an initial set of partons, in the Lund string fragmentation model. It was derived from classical probability concepts but has later been interpreted as the result of gauge invariance in terms of the Wilson gauge loop integrals. In this paper we will present a general method to implement the area law for a multi-gluon string state. In this case the world surface of the massless relativistic string is a geometrically bent $(1+1)$-dimensional surface embedded in the $(1+3)$-dimensional Minkowski space. The partonic states are in general given by a perturbative QCD cascade and are consequently defined only down to a cutoff in the energy-momentum fluctuations. We will show that our method defines the states down to the hadronic mass scale inside an analytically calculable scenario. We will then show that there is a differential version of our process which is closely related to the generalized rapidity range λ, which has been used as a measure on the partonic states. We identify λ as the area spanned between the directrix curve (the curve given by the parton energy-momentum vectors laid out in colour order, which determines the string surface) and the average curve (to be called the $\mathcal{P}$-curve) of the stochastic X-curves (curves obtained when the hadronic energy-momentum vectors are laid out in rank order). Finally we show that from the X-curve corresponding to a particular stochastic fragmentation situation it is possible to reproduce the directrix curve (up to one starting vector and a set of sign choices, one for each hadron). This relationship provides an analytical formulation of the notion of parton–hadron duality. The whole effort is made in order to get a new handle to treat the transition region between where we expect perturbative QCD to work and where the hadronic features become noticeable.

1 Introduction

The Lund string fragmentation model was developed many years ago [1,3] and as implemented in the well-known Monte Carlo simulation program JETSET [4] it has been very successful in reproducing experimental data from high energy multi-particle processes.

The model is based on a few general assumptions:

(i) the final state particles stem from the break-up of a string-like force field spanned between the coloured constituents,
(ii) there is causality and Lorentz invariance, and
(iii) the production of the particles can be described in terms of a stochastic process which obeys a saturation assumption. We have, in a recent paper [5], re-derived the major result for the $(1+1)$-dimensional model, which is applicable for events with a quark (q, a colour-3) and an antiquark ($\bar{q}$, a colour-$\bar{3}$) at the endpoints of the string but with no interior gluonic (g, colour-8) excitations. The result is that the (non-normalized) probability for the production of an n-particle final state of hadrons with energy-momenta $\{p_j\}$ and masses $\{m_j\}$ is given by the Lund area law:

$$\mathrm{d}P_n(\{p_j\};P_{\mathrm{tot}}), = \prod_{j=1}^{n} N_j d^2p_j \delta(p_j^2 - m_j^2) \times \delta\left(\sum_{j=1}^{n} p_j - P_{\mathrm{tot}}\right) \exp(-bA), \quad (1)$$

where A is the area spanned by the string "before" the break-up, cf. Fig. 1, P_{tot} is the total energy-momentum of the state and $\{N_j\}$ and b are parameters related to the density of hadronic states and the break-up properties of the string field, respectively.

The result in (1) is evidently similar to a quantum mechanical transition probability. It is the final state phase space multiplied by a squared matrix element, which in this case would correspond to the negative area exponential. In [5] we have shown that it is possible to "diagonalize" the model, i.e. to express the result in (1) as a product of (diagonal) transition operators (in quantum mechani-

[a] e-mail: bo@thep.lu.se
[b] e-mail: sandipan@thep.lu.se
[c] e-mail: fredrik@thep.lu.se

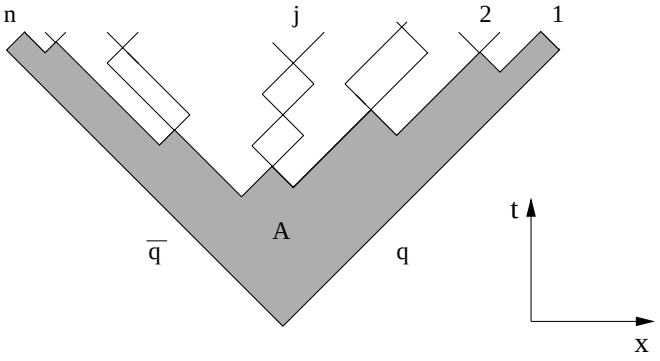

Fig. 1. A high-energy string break-up

cal language it would correspond to density operators). It turns out that in this way the dynamics can be described in terms of $(1+1)$-dimensional (space-like) harmonic oscillators.

Shortly after the original derivation of the area law [1] Sjöstrand [6] provided an implementation of the model applicable also for multi-gluon states, i.e. when the string surface is no longer flat but geometrically bent due to the internal excitations. Sjöstrand's method is to project the positions of the break-up points (the vertices) from the (flat) $(1+1)$-dimensional model as given by (1) onto the surface of the bent string. The projection is done so that the proper times of the vertices and the squared masses of the particles produced between them are the same. Unfortunately this method does not fulfil the area law on the bent surface because it is a geometrical fact that the areas "below the vertices" are not invariant under such a projection from a flat to a bent surface.

Although the area law is not fulfilled on an event to event basis by the method in [6] we will show that it is fulfilled in an average sense, i.e. the predicted inclusive distributions are little affected by the differences. It is well known that the experimental results for these distributions are well described by JETSET even up to the largest available energies of today.

The intention of this note is to implement another method for particle production in multi-gluon states which fulfils the area law at every single step in the production process. We will find that it is necessary to tackle a set of problems in the definition of the states which we apply the process to. We note that the states defined by perturbation theory are resolved only to the scale of some virtuality cutoff. We will find that our method provides a set of excitations on the hadronic mass scale, in the string field. We will investigate the properties of these "soft hadronization gluons" in future work.

The states of the massless relativistic string fulfil a minimum principle, i.e. the surface spanned in spacetime by the string during its motion is a minimal surface. This means on the one hand, that the states should be stable against small-scale variations and on the other hand that the surface is fully determined by the boundary curve. In this case the boundary curve corresponds to the orbit of one of the endpoints, conventionally chosen as the q-endpoint. Therefore, the process we are going to define is a process along this curve, to be called the *directrix curve*, which is completely defined by the perturbative cascade. In this paper we will treat the partons as massless, although both the process and the directrix curve can be defined for a general case with massive quarks.

One property which can be derived from (1) is that the average decay region is a typical hyperbola. On the average, the final state hadrons in our process will be produced in the same way, albeit this time along a set of connected hyperbolae. In [2] we have defined such an average curve and we will, in this paper, call it the $\mathcal{X}$-curve. Just as a simple hyperbola has a length proportional to the hyperbolic angle that it spans (this corresponds to the available rapidity range along the mean decay region, in a two-jet system of hadrons) the $\mathcal{X}$-curve has a length corresponding to a generalized rapidity range, usually called the λ measure [2,3]. The $\mathcal{X}$-curve is defined in terms of differential equations and we will show the close relationship between the $\mathcal{X}$-curve and our process in the limit of a vanishing hadron mass.

There are several reasons to undertake this investigation. One is to compare the precise implementation of the area law to the approximate process in [6]. We will do this both in this paper and in future publications.

Another reason is to get a handle on the general structure of fragmentation, in particular to be able to treat also the multi-gluon fragmentation states by the analytical methods introduced in [5]. This is of particular interest for the transition region, i.e. the region in between where we expect perturbation theory to work and where we know that the non-perturbative fragmentation sets in.

A final reason is to investigate the stability of the states in QCD under fragmentation, i.e. given a multi-gluon state defined according to the rules of perturbation theory (with cutoffs as mentioned above) to find out to what extent it can be modified so that the observable results after fragmentation are still in agreement with the experiments. In the Lund interpretation of fragmentation where the particles stem from the energy of the force field, it is tacitly assumed that modifications of the perturbative state below and up to the scale of the hadronic masses should have no effects. We will find that it is necessary to take into account the coherence properties of the radiation in any modification.

Although the methods presented in this paper are applicable to any multi-gluon state, for definiteness we will concentrate on the states obtained in e^+e^--annihilation processes where we expect an original colour singlet $(q\bar{q})$-state to form and start to go apart, producing a set of bremsstrahlung gluons inside an essentially point-like region. We will also be satisfied to treat a single kind of hadron with mass m. Finally, in this paper we will not introduce gaussian transverse momentum fluctuations (which we expect in a tunneling scenario [3]) in the fragmentation process. We will investigate the influence of such fluctuations in a future publication.

In Sect. 2, we provide a set of necessary formulae from the $(1+1)$-dimensional Lund model. In Sect. 3, we consider the motion of strings containing internal excitations.

We also provide a description of the coherence properties of QCD and some necessary formulae to understand the $\mathcal{X}$-curve. In Sect. 4, we define the properties of the string break-up in general. We find that the most general implementation of the area law leads to a highly intractable process and therefore in Sect. 5 we define another approach which mends all the problems with the earlier one. In particular, in Sect. 5.3 we show a close relationship between a differential version of this process and the $\mathcal{X}$-curve. In Sect. 6, we present a set of results from our method, followed by some concluding remarks on future work in Sect. 7.

2 Some results from the $(1+1)$-dimensional model

2.1 The area law

The Lund model contains a non-trivial interpretation of the QCD force field in terms of the massless relativistic string with the quarks (q) and the antiquarks ($\bar{q}$) at the endpoints and the gluons (g) as internal excitations on the string field. It is assumed that the force field can break up into smaller parts in the fragmentation process by the production of new ($q\bar{q}$)-states (i.e. new endpoints). A q from one such break-up point ("vertex"), together with a $\bar{q}$ from an adjacent vertex and the field between them, can form a hadron on mass shell.

For the simple case when there are no gluons, the string field only corresponds to a constant force field (with a phenomenological size $\kappa \simeq 1\,\mathrm{GeV/fm}$) spanned between the original $q\bar{q}$-pair. In a semi-classical picture, conservation of energy-momentum allows the creation of a new massless pair at some point along the field. The pair will then go apart along opposite light-cones, using up the energy in the field in between (in this way the confined fields will always end on the charges). In order that the hadron produced between two adjacent vertices should have a positive squared mass, it is necessary that the vertices are placed in a space-like manner with respect to each other. Consequently, time-ordering will be a frame-dependent statement (in any Lorentz frame the slowest particles will be the first to be produced, thereby fulfilling the requirements in a Landau–Pomeranchuk formation time scenario). It is possible to order the production process instead, along the light-cones and introduce the notion of *rank* so that the first rank hadron along the original q-light-cone will contain that q together with a $\bar{q}$ from the first vertex along the light-cone, the second rank hadron a q from the first vertex and a $\bar{q}$ from the next etc.; cf. Fig. 1. Rank-ordering is a frame-independent procedure. It is of course possible to introduce a rank-ordering also from the end containing the original $\bar{q}$.

One obtains [1,3,5] the unique process described by (1) from these observations and an assumption that the break-up process obeys a saturation assumption, i.e. that after many steps when we are far from the endpoints the proper times of the vertices will be distributed according to an energy-independent distribution.

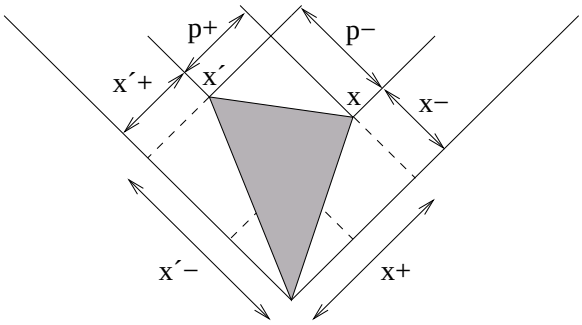

Fig. 2. Two adjacent vertices of the string break-up process

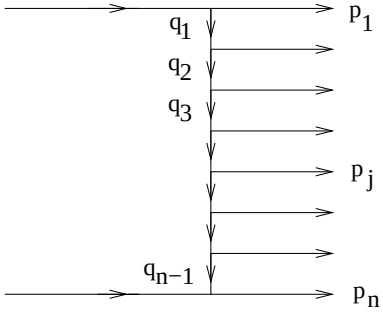

Fig. 3. A ladder diagram describing multi-particle production

A particular feature is that if a particle with energy-momentum $p = (p_+, p_-)$ and with squared mass $m^2 = p^2 = p_+p_-$ is produced between the two vertices with $x = (x_+, x_-)$ and $x' = (x'_+, x'_-)$ then we have (cf. Fig. 2)

$$\begin{aligned} p_+ &= \kappa(x_+ - x'_+) \equiv q_+ - q'_+, \\ p_- &= \kappa(x'_- - x_-) \equiv q_- - q'_-. \end{aligned} \tag{2}$$

Thus we find that on a flat string surface the difference between the vertex points will fulfil:

$$(x - x')^2 = -m^2/\kappa^2. \tag{3}$$

(2) implies that the $(1+1)$-dimensional Lund fragmentation model may also be described by means of a multi-peripheral chain diagram as in Fig. 3 or in an energy-momentum space picture as in Fig. 4.

This is used in [5] in order to subdivide the area law process into steps in between the vertices. The energy-momentum conserving δ-distribution in (1) can be "solved" by introducing the momentum transfers $\{q_j\}$ instead of the hadron momenta $\{p_j\}$. Then the mass-shell condition means that the hyperbolic angle between the vertices and the size of the area slit, exhibited in Fig. 2 are fixed by the squared sizes $q^2 = -\Gamma$, $(q')^2 = -\Gamma'$ and $(q - q')^2 = m^2$. The result is that (1) can be rewritten as a product of steps between the $\{\Gamma_j\}$:

$$\begin{aligned} \mathrm{d}P_n(\{p_j\}, P_{\mathrm{tot}}) &= \prod K(\Gamma_j, \Gamma_{j-1}, m^2) d\Gamma_j, \\ K(\Gamma, \Gamma', m^2) &= N \frac{\exp\left(-\frac{b}{2}\sqrt{\lambda(\Gamma, \Gamma', -m^2)}\right)}{\sqrt{\lambda(\Gamma, \Gamma', -m^2)}}, \\ \lambda(a, b, c) &= a^2 + b^2 + c^2 - 2ab - 2ac - 2bc. \end{aligned} \tag{4}$$

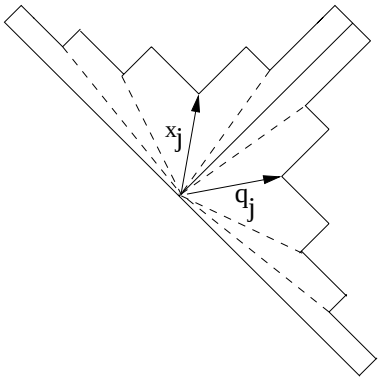

Fig. 4. The energy-momentum space picture (q_j) and the spacetime picture (x_j) respectively

It is a remarkable fact that the transfer operators K can be diagonalized in terms of the eigenfunctions of the harmonic oscillator (those which are boost invariant in a $(1+1)$-dimensional space-like Minkowski space; in a two dimensional euclidean space they correspond to a vanishing angular momentum) $g_n(\Gamma)$ with the eigenvalues solely determined by the squared mass of the hadrons produced in between:

$$K(\Gamma,\Gamma',m^2)=\sum_{n=0}^{\infty} g_n(\Gamma)\lambda_n(m^2)g_n(\Gamma'). \tag{5}$$

The eigenvalues λ_n are analytic continuations of the harmonic oscillator eigenfunctions to time-like values of the argument, [5]. Useful representations of K and the eigenvalues λ_n are

$$\begin{aligned} K(\Gamma,\Gamma',m^2) &= \int_0^1 \frac{\mathrm{d}z}{z}\exp\left(-\frac{b}{2}\left(z\Gamma+\frac{m^2}{z}\right)\right) \\ &\quad\times\delta\left(\Gamma'-(1-z)\left(\Gamma+\frac{m^2}{z}\right)\right), \\ \lambda_n(m^2) &= N\exp\left(\frac{bm^2}{2}\right)\int_0^1\frac{\mathrm{d}z}{z}(1-z)^n \\ &\quad\times\exp\left(-\frac{bm^2}{z}\right). \end{aligned} \tag{6}$$

We have introduced the positive light-cone fraction of the produced hadron z defined by $(x_+ - x'_+) = zx_+$. It is straightforward algebra to prove that the shaded area, exhibited in Fig. 2 is given by the exponent $(1/2)(z\Gamma + (m^2/z))$ in the representation of the kernel K. We also note that the area obtained by summing the areas of the regions marked I, II and III in Fig. 5 is equal to twice this area and that m^2/z equals the sum of the areas of regions I and II. There is a simple relationship between the two adjacent values of Γ in the representation of K:

$$\Gamma'=(1-z)\left(\Gamma+\frac{m^2}{z}\right). \tag{7}$$

Finally we note the identity (in easily understood notation)

$$(I)(III)=(II)(IV). \tag{8}$$

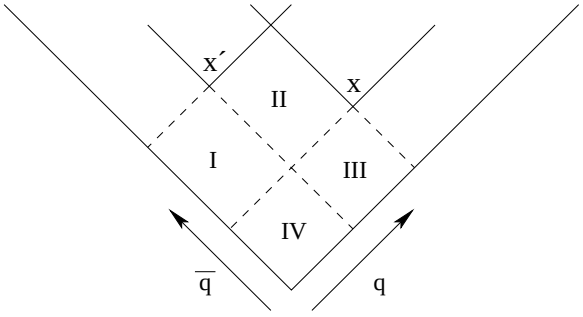

Fig. 5. The figure shows the two vertices and the regions I, II, III and IV described in the text

Equation (8), just as (3), is only valid for a flat string surface and a particular consequence is that the region IV is non-vanishing for the $(1+1)$-dimensional model. As the area of the region IV is proportional to $(1-z)$, the variable z must always be smaller than unity, i.e. there is a built in requirement that a typical step of the process can never use up all the available light-cone energy-momentum.

Such a requirement also comes out of the following argument. Suppose that we would integrate $\mathrm{d}P_n$ in (1) over all possible energy-momenta and then sum over all multiplicities. Due to Lorentz invariance, we will obtain a function $R(s)$ which can only depend upon the total squared energy-momentum $s = P^2_{\mathrm{tot}}$. If we pick out the dependence on the first particle and sum and integrate over all the rest we obtain an integral equation for the function R:

$$\begin{aligned} R(s) &= (\mathrm{B.T.}) + \int_0^1 N\frac{\mathrm{d}z}{z}\exp\left(-b\frac{m^2}{z}\right)R(s'), \\ s' &= (1-z)\left(s-\frac{m^2}{z}\right), \end{aligned} \tag{9}$$

where (B.T.) stands for "boundary condition term" and the variable s' is equal to the squared mass of all the remaining particles if the first hadron takes the light-cone fraction z (we note the similarity to (7)). The integral equation (9) has an asymptotic solution $R \propto s^a$ (with the parameter a being a function of N and bm^2, cf. [5]) with the requirement

$$\int_0^1 N\frac{\mathrm{d}z}{z}(1-z)^a\exp\left(-b\frac{m^2}{z}\right)=1. \tag{10}$$

Consequently while the exclusive formula for the production of a particular hadron with the light-cone fraction z is given by the area law, the inclusive probability to produce this hadron (irrespective of what comes after it in the process) must be weighted with $R(s')/R(s) \simeq (1-z)^a$. Therefore, the well-known Lund fragmentation formula is given by the integrand in (10) and there is a power suppression for large values of the fragmentation variable.

The formulae presented above correspond to an ordering along the positive light-cone, i.e. the variable z is defined as the positive light-cone momentum fraction of the particle. It is possible to redefine everything in terms

of an ordering along the negative light-cone, i.e. to introduce the corresponding negative light-cone component ζ by writing $(x'_- - x_-) = \zeta x'_-$. It is straightforward to prove that

$$\zeta = \frac{m^2}{m^2 + z\Gamma} \text{ and } z = \frac{m^2}{m^2 + \zeta\Gamma'}, \tag{11}$$

and from this we find that the integrand in the representation of the kernel K can be reformulated from $(z, \Gamma) \to (\zeta, \Gamma')$ to exhibit the symmetry between the descriptions along the positive and the negative light-cone directions

$$\begin{aligned} &\frac{\mathrm{d}z}{z}\delta\left(\Gamma' - (1-z)\left(\Gamma + \frac{m^2}{z}\right)\right) \\ &\quad \times \exp\left(-\frac{b}{2}\left(z\Gamma + \frac{m^2}{z}\right)\right), \\ &\to \frac{\mathrm{d}\zeta}{\zeta}\delta\left(\Gamma - (1-\zeta)\left(\Gamma' + \frac{m^2}{\zeta}\right)\right) \\ &\quad \times \exp\left(-\frac{b}{2}\left(\zeta\Gamma' + \frac{m^2}{\zeta}\right)\right). \end{aligned} \tag{12}$$

3 The description of a multi-gluon string state

The dynamics of the massless relativistic string is based upon the principle that *the surface spanned by the string during its motion is a minimal surface*. This means that *the surface is completely determined by its boundary*. In the Lund model the string is used as a model for the confined colour force field in QCD and the above property then has the further important implication that the dynamics will be infrared stable, i.e. *all predictable features from the decay of the force field should be stable against minor deformations of the boundary*.

For an open string a single wave moves across the spacetime surface and bounces at the endpoints. *The wave motion is determined by a (four-)vector-valued shape function, which we will call the directrix,* $\mathcal{A}$. Thus a point on the string, parametrized by the amount of energy σ, between the point and (for definiteness) the q-endpoint is, at the time t, at the position

$$x(\sigma, t) = \frac{1}{2}\left(\mathcal{A}\left(t + \frac{\sigma}{\kappa}\right) + \mathcal{A}\left(t - \frac{\sigma}{\kappa}\right)\right). \tag{13}$$

We will from now on put the string constant κ equal to unity in order to simplify the formulae.

While the tension $\boldsymbol{T} = \partial\boldsymbol{x}/\partial\sigma$ is directed along the string, the velocity $\boldsymbol{v} = \partial\boldsymbol{x}/\partial t$ is directed transversely so that $\boldsymbol{T} \cdot \boldsymbol{v} = 0$. The definition of σ also implies that $\boldsymbol{T}^2 + \boldsymbol{v}^2 = 1$ (all the three-vector relations are valid in the local rest frame). Together this means that the directrix function has an everywhere light-like tangent

$$\left(\frac{\mathrm{d}\boldsymbol{\mathcal{A}}}{\mathrm{d}\xi}\right)^2 = 1 = \left(\frac{\mathrm{d}\mathcal{A}_0}{\mathrm{d}\xi}\right)^2. \tag{14}$$

The tension must vanish at the endpoints ($\sigma = 0$ and $\sigma = E_{\mathrm{tot}}$) and this implies that the directrix must be a periodic function with the property

$$\mathcal{A}(\xi + 2E_{\mathrm{tot}}) = \mathcal{A}(\xi) + 2P_{\mathrm{tot}}, \tag{15}$$

where P_{tot} (E_{tot}) is the total energy-momentum (energy) of the state. While according to (13), the directrix $\mathcal{A}(t)$ describes the motion of the q-end, from (15) it is evident that

$$\mathcal{A}_{\bar{q}}(t) = \mathcal{A}(t + E_{\mathrm{tot}}) - P_{\mathrm{tot}}, \tag{16}$$

will describe the motion of the $\bar{q}$-end. Finally, if the string starts out from a point (at the time $t = 0$) then we must have the symmetry

$$\mathcal{A}(\xi) = -\mathcal{A}(-\xi). \tag{17}$$

Using the Lund interpretation of the gluons as internal excitations on the string it is easy to construct the first half period of the directrix curve: it starts with the quark energy-momentum k_1 and then the gluon energy-momenta $\{k_j\}$ are laid out in colour order and it ends with the $\bar{q}$ energy-momentum k_n, for a string with $(n-2)$ gluons. In this way the q-endpoint will be acted upon by the colour-ordered excitations as they arrive in turn. From (15) and (17) it follows that we obtain the directrix of the second half period by reversing the order, starting with the $\bar{q}$ energy-momentum and ending with the q energy-momentum (besides the translation this is the way the $\bar{q}$-endpoint will move according to (16)).

The energy-momentum content in the string at a certain time t, between the point σ and the q-end is given by

$$\int_0^\sigma \mathrm{d}\sigma' \frac{\partial x}{\partial t} = \frac{1}{2}(\mathcal{A}(t+\sigma) - \mathcal{A}(t-\sigma)). \tag{18}$$

3.1 The coherence conditions in QCD

The properties of the directrices which are described above are common to all states of the massless relativistic string. On the other hand the use of the string as a model for the force fields of QCD may single out a particular class of all possible states. We will briefly discuss *the conditions which correspond to the coherence conditions of bremsstrahlung radiation in a gauge field theory*.

Multi-gluon radiation is in general described by means of perturbative cascade models. In order to consider the properties of the states, we will make use of the ideas behind the Lund dipole model. To see the emergence of a multi-gluon state we start out with the following two basic results from QCD bremsstrahlung, (cf. [3,7,8]).

[B1] The original $(q\bar{q})$-state emits bremsstrahlung radiation according to the ordinary dipole formula, i.e. there is an inclusive density of gluon quanta which is flat in rapidity y and the logarithm of the squared transverse momentum $\kappa = \ln(k_\perp^2)$ with a density given by the coupling, $\bar{\alpha} \equiv C\alpha_{\mathrm{s}}/2\pi$:

$$\mathrm{d}n = \bar{\alpha}\mathrm{d}\kappa\mathrm{d}y. \tag{19}$$

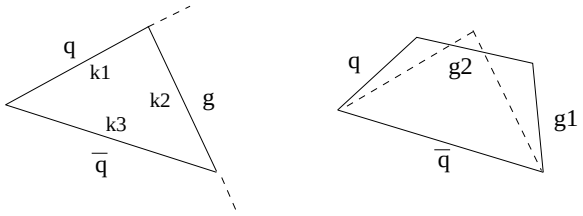

Fig. 6. The emission of the first and the second gluon respectively

[B2] After the first ("hardest") gluon (g_1) is emitted there are two dipoles available, one between the (qg_1) and one between the $(g_1\bar{q})$ with squared masses $s_{12} \equiv (k_q + k_{g_1})^2$ and $s_{23} \equiv (k_{g_1} + k_{\bar{q}})^2$. The second gluon may be emitted independently inside the angular (rapidity) range of the first or the second dipole. We note that the two dipoles (each spanned by two light-like parton energy-momenta) move apart in the total cms.

After the emission of the second gluon, according to the Lund dipole model [8], there are three independent dipoles for further emission, and so on. The masses of the dipoles will quickly decrease and therefore also the transverse momentum size of the emitted gluons. The cascades are stopped by some "virtuality" cutoff, either in the dipole mass or in the transverse momentum. The dipole model is implemented in the Monte Carlo simulation program ARIADNE [9].

In terms of the directrix, the original state is described by the light-like energy-momenta of the original $(q\bar{q})$-pair. After the emission of the first gluon the state, in space (in the c.m.s.), will be described by a (connected) triangle, cf. Fig. 6, where the vectors $\boldsymbol{k}_q \equiv \boldsymbol{k}_1$ and the vectors $\boldsymbol{k}_g \equiv \boldsymbol{k}_2$ constitute one of the dipoles and the $\boldsymbol{k}_2$ and $\boldsymbol{k}_{\bar{q}} \equiv \boldsymbol{k}_3$ the second dipole, as discussed above. (We note that for light-like vectors the space part length is equal to the time component.) Emission of the second gluon will then occur in between the two vectors describing the dipole and this evidently means that the second gluon vector will "cut off" one of the triangular corners, making the directrix into a quadrangle etc. (Note that already with the emission of two gluons, the vectors shown in Fig. 6 no longer need to be in a plane.)

In general, there will be an emission of a set of "hard" gluons which will determine the general shape of the directrix. The remaining emissions will then make the directrix smoother and smoother as each new emission will correspond to a gluon vector which cuts off an earlier corner. This means that the angle between the energy-momentum vectors of colour-connected partons becomes smaller (along the main directions, determined by the hard emissions) the longer the cascade continues. This is the way that the coherence properties of the bremsstrahlung radiation work, and it is sometimes referred to as the "strong angular condition". Later on, we will find that this angular condition will play an important role when we consider the deviations in the partonic states which are allowed by the fragmentation process.

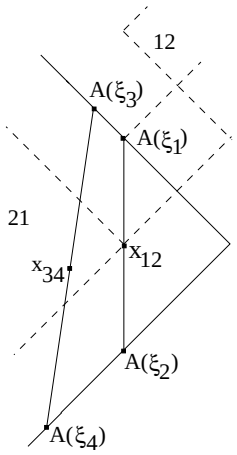

Fig. 7. The system (12) is shown as a string piece which is moving away, while the system (21) is translated to x_{12}. The second break-up point x_{34} is the middle point between $A(\xi_3)$ and $A(\xi_4)$. In this way, the particle produced in between x_{12} and x_{34} can be taken either as the second particle in the break-up of the original system or the first in the system (21)

4 The general break-up of a string field

We will now consider the partitioning of a general string state at a point $x(\sigma, t)$ and after that define the most general process possible for the area law.

According to (13) the break-up will occur at the middle point $(1/2)(\mathcal{A}(\xi_1) + \mathcal{A}(\xi_2))$ between two positions on the directrix, determined by $\xi_1 > \xi_2$ with $t = (1/2)(\xi_1 + \xi_2)$ and $\sigma = (1/2)(\xi_1 - \xi_2)$, cf. Fig. 7. There will be two parts of the string left over and we will now describe their motion after the break-up.

The first part (to be denoted "(12)") can be described by the "new" directrix $\mathcal{A}_{12}(\xi) \equiv \mathcal{A}(\xi)$ for $\xi_2 \le \xi \le \xi_1$. It will contain the energy-momentum $P_{12} = (\mathcal{A}(\xi_1) - \mathcal{A}(\xi_2))/2$, cf. Fig. 7, so that it can be continued as in (15) with $P_{\rm tot} \to P_{12}$. Starting it out from the position $\mathcal{A}_{12}(\xi_2) \equiv \mathcal{A}(\xi_2)$, it is the "new" orbit of the (original) q-particle in the string (12). To obtain the corresponding orbit for the "new" $\bar{q}$-end we use (16) to obtain $\mathcal{A}_{12\bar{q}} \equiv \mathcal{A}_{12}(t + (\xi_1 - \xi_2)/2) - P_{12}$. If we start at the "break-up" time $t = (1/2)(\xi_1 + \xi_2)$, it will evidently behave just as if we had adjoined the directrix $\mathcal{A}_{12}$ to the point $x(\sigma, t)$ (note that $\mathcal{A}_{12}(\xi_1) = 2P_{12} + \mathcal{A}_{12}(\xi_2)$).

The second part (denoted "(21)") can be described as the remainder, i.e. $\mathcal{A}_{21} = \mathcal{A}(\xi)$ with $\xi_1 \le \xi \le 2E_{\rm tot} + \xi_2$ (noting that the original directrix is continued according to (15)). The directrix $\mathcal{A}_{21}$ contains the energy $P_{21} = P_{\rm tot} - P_{12}$ and is continued accordingly. To find the orbit of the produced q-end in the part (21) we adjoin the directrix $\mathcal{A}_{21}$ to the point $x(\sigma, t)$ starting it at $\xi = \xi_1$. The (original) $\bar{q}$ will again move according to (16).

The most noticeable property is that for a multi-gluon force field the directrices of the two new string parts will not fulfil (17). This implies that the endpoints of the new strings never meet but instead turn around each other so that each of the two states will contain angular momentum. *It is only in the* (1+1)*-dimensional case that the two*

new string parts will have the same properties as the original string (though they will be scaled down in size and have different rest frames due to the momentum transfer at the break-up). The conclusion is that *the final state in a multi-gluon string fragmentation in general depends upon the ordering of the different break-ups.*

4.1 A general process based upon the area law

We may nevertheless devise a string breaking process on a "frozen" string surface, i.e. under the assumption that the string surface is once and for all a given device (this is also the way Sjöstrand treated the problem exhibited above). Assume that the system (12) is a hadron on the mass shell, produced as the "first" hadron along the original q-direction (i.e. the point $\mathcal{A}(\xi_2)$ is along the q energy-momentum vector and $\mathcal{A}(\xi_1)$ on the other side of the corner in the directrix between the q and the first gluon). Then we may choose two new points $\xi_3 > \xi_1$ and $\xi_4 < \xi_2$ to obtain the second rank hadron (34) with energy-momentum $p_{34} = (1/2)(\mathcal{A}(\xi_3) - \mathcal{A}(\xi_1) + \mathcal{A}(\xi_2) - \mathcal{A}(\xi_4))$ with the production vertex at $x_{34} = (1/2)(\mathcal{A}(\xi_3)+\mathcal{A}(\xi_4))$. We may evidently continue this process across the string surface, and we note that at every step it is only necessary to choose two numbers: $(\delta\xi)_+ = \xi_3 - \xi_1$ and $(\delta\xi)_- = \xi_2 - \xi_4$. They must be chosen so that the corresponding p_{34} is the energy-momentum of a particle on the mass shell. It is necessary to have a second condition, however, and we may then use the area law.

For the $(1+1)$-dimensional model the numbers $(\delta\xi)_\pm$ evidently correspond to the light-cone coordinates z and ζ in Sect. 2. The indices $\pm$ can be given a further meaning for the general directrix. According to (13) there is a left-moving and a right-moving wave spanning the string surface and according to (15) the fixed phase parts (from now on we will call them "grains") "stream" across and bounce back (thereby turning from left- to right-movers) at the q and $\bar{q}$ ends.

We may describe the situation in a (σ, t)-plane, cf. Fig. 8, with the right- and left-moving grains moving along fixed "light-cone lines". The whole string is, at the time $t = 0$, gathered into a single point at the origin. The boundary values at $\sigma = 0$ and $\sigma = E_{\rm tot}$ are the directrix $\mathcal{A}(t)$ and the orbit of the $\bar{q}$, i.e. $\mathcal{A}_{\bar{q}}(t)$, respectively. A break-up point $x \equiv x_{12}$ is reached by the meeting of the left-moving grain indexed ξ_1 and the "right-mover" ξ_2 and the break-up at x_{34} by the left-mover ξ_3 and right-mover ξ_4. The energy-momentum p_{34}, streaming into the hadron produced between x_{12} and x_{34}, is evidently $(1/2)(\mathcal{A}(\xi_3) - \mathcal{A}(\xi_1))$ from the left and $(1/2)(\mathcal{A}(\xi_2) - \mathcal{A}(\xi_4))$ from the right. If we use $\pm$ as indices for the left- and the right-movers respectively we obtain a useful parametrization.

With regard to surface areas there is an obvious (scalar) surface element defined by the surface spanned by the (incremental) grains coming from the left and the right.

$$\mathrm{d}A \propto \mathrm{d}\mathcal{A}_+ \cdot \mathrm{d}\mathcal{A}_-. \tag{20}$$

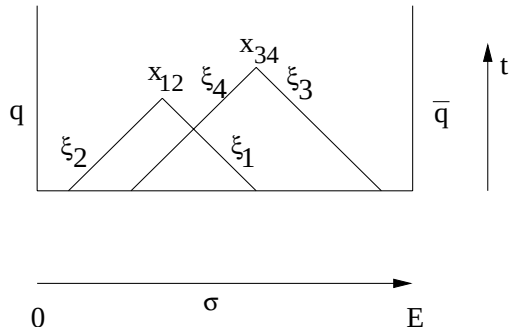

Fig. 8. The break-up points and the corresponding right and left-moving grains in the (σ,t)-plane, as described in the text

Using this we may easily calculate the area "below the vertices" x_{12} and x_{34} (cf. Fig. 8) as they are defined above. They are the correspondence to the squared proper times Γ considered in Sect. 2 (in the Fig. 5 they would correspond to the areas $I + IV$ and $III + IV$).

$$\Gamma_{12} = x_{12}^2 \text{ and } \Gamma_{34} = x_{34}^2. \tag{21}$$

So, for the vertices shown in Fig. 8, these areas are just the squared proper times of the vertices. But we note that they cannot be expressed as the products of light-cone components or even in terms of products of sets of left- and right-movers solely, for general multi-gluon strings.

The area below the vertices (if we neglect the squared mass term in the area law, which can evidently be included in the normalization constants N in (1)) can be expressed as

$$A_{1234} = x_{12}^2 + x_{34}^2 - x_{14}^2. \tag{22}$$

(this is the correspondence to the area called $I + III + IV$ in connection with (8)). We note that the area corresponding to IV, i.e. x_{14}^2 in (22), may vanish in this case, i.e. the left-mover indexed 1 and the right-mover indexed 4 may meet "before" $t = 0$. This means that the condition in (8) cannot be met for the general situation.

We may nevertheless include these considerations to devise an exact version of the area law in (1). We write, in an obvious way, the differentials $\mathrm{d}^2p \to (\mathrm{d}p_+ \cdot \mathrm{d}p_-)$ and include the mass-shell condition by a δ-distribution as in (1). The result is, however, very complex to treat and for our purposes there are three shortcomings:

1. If we treat the process in an iterative way, at every step, just as we mentioned above, there are two numbers $(\delta\xi)_\pm$ to be solved for. One is fixed by the mass-shell condition and the other can be fixed by the area exponential; but the distribution functions are very complex (cf. the remarks under 2 below). In principle everything can be done by Monte Carlo simulation methods but even with very fast computers and the best possible computer routines this model will always be much slower than a process where there is only one number to be solved for, at every step.
2. Due to the complexity of the formulae there is no way we can obtain useful analytical tools to study the be-

havior of the correspondences to the transition operators as in e.g. (5). This also implies that there is no way that we can define the total integral and sum over the produced hadronic states (as we could do for the $(1+1)$-dimensional model in (9) and (10)) so as to be able to obtain the correct weighting in every step of an inclusive cascade.

3. Although this implementation of the area law is an "exact" procedure, fulfilling at every step the mass-shell condition and taking the "true" area below the vertices into account, it nevertheless starts out from the assumption that the partonic state is so well defined that there are reasons to implement an "exact" theoretical fragmentation procedure on it. This is in general not the case, i.e. the partonic state defined by perturbation theory is only well defined down to some virtuality cutoff as we have discussed before.

We use quotation-marks on the word "exact" in order to indicate that the use of a "frozen surface" is in itself an assumption introduced to mend the problems obtained from the use of classical physics and neglect of the subsequent angular momentum production. In the third item above, we are coming back to the statement at the beginning of the section, that infrared stability should imply that minor deformations of the boundary (in this case changes in the partonic state as defined by the directrix $\mathcal{A}$ up to the order of the hadronic mass scales) should not be noticable in the results. In the next section we will define a procedure which will mend all the three shortcomings mentioned above.

5 The Lund string fragmentation as a process along the directrix

In this section, we will consider a fragmentation process which is defined along the directrix and does not suffer from the three problems considered at the end of Sect. 4.1. In order to exhibit the idea we will start with the $(1+1)$-dimensional model and rewrite it in a useful way. After that we will extend it to the general case. In particular, we will allow modifications of the order of the hadronic mass scale in the directrix in accordance with the discussion under point 3 above.

5.1 The directrix process for the $(1+1)$-dimensional case

In this case the directrix contains only two directions, given by the $\bar{q}$ energy-momentum vector (to be called $\mathcal{A}_+$ in accordance with the notation introduced in Sect. 4.1) and the q energy-momentum ($\mathcal{A}_-$). A vertex point x_j, obtained after the production of j hadrons from the q-side, $p_1, \ldots, p_j$ is then described (with respect to the origin) by

$$x_j = \frac{1}{2}(\mathcal{A}_{+j} + \mathcal{A}_{-j}). \tag{23}$$

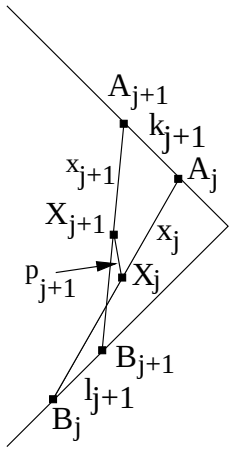

Fig. 9. A description of the fragmentation process along the directrix with notations according to the text

We also know that

$$\sum_1^j p_\ell = \frac{1}{2}(\mathcal{A}_{+j} - \mathcal{A}_{-j}). \tag{24}$$

Using the symmetry of a directrix passing through a single point (see (17)) we may find another point on the directrix with the property

$$\mathcal{A}_{-j} \equiv \mathcal{A}_-(\xi_j) = -\mathcal{A}_-(-\xi_j) \equiv -\mathcal{B}_{-j}. \tag{25}$$

We will from now on drop the indices $\pm$ on $\mathcal{A}_+$ and $\mathcal{B}_-$ but we note that they do describe points on the same directrix in accordance with the left- and right-mover notation in Sect. 4.1. While $\mathcal{A}_-$ goes "backward" for increasing j-values, $\mathcal{B}$ follows the q-direction.

We may now consider the hadron energy-momenta to define a curve from the origin "along the directrix" such that after j steps it has reached the point

$$\sum_1^j p_\ell \equiv X_j = \frac{1}{2}(\mathcal{A}_j + \mathcal{B}_j), \tag{26}$$

while the difference between the point $\mathcal{A}_j$ on the directrix and X_j is given by x_j in (23). The production of a new particle p_{j+1} then corresponds to choosing two new points X_{j+1} and $\mathcal{A}_{j+1}$ (along the directrix) such that, cf. Figure 9

$$X_{j+1} - X_j = p_{j+1} \text{ and } \mathcal{A}_{j+1} - \mathcal{A}_j \equiv k_{j+1}. \tag{27}$$

We also obtain a new "vertex" vector x_{j+1} by the identity (cf. Fig. 9):

$$p_{j+1} + x_{j+1} = x_j + k_{j+1}. \tag{28}$$

In this way the vertex vector fulfils $x_{j+1} = \mathcal{A}_{j+1} - X_{j+1}$ just as $x_j = \mathcal{A}_j - X_j$. We have then arranged it so that the hadrons are produced along a curve, the X-curve, from the origin and the vertex vectors are the connectors for this curve going from the produced particle to the directrix. Before we consider the area law in this situation we note

the symmetry between a reversed process and the process described above, i.e. when we go from X_j to X_{j+1} producing p_{j+1} by the use of a part k_{j+1} of the directrix along $\mathcal{A}$.

To see the reverse process we note that the vector x_j can just as well be reached by taking the difference between the point X_j on the hadron curve, (26), and "the backward point" on the directrix $\mathcal{B}_j$.

$$x_j = \frac{1}{2}(\mathcal{A}_j - \mathcal{B}_j) = \mathcal{A}_j - X_j = X_j - \mathcal{B}_j. \tag{29}$$

Using this we could evidently consider the production of the particle p_{j+1} as a step from $\mathcal{B}_j$ to $\mathcal{B}_{j+1} = \mathcal{B}_j + \ell_j$ (cf. (27)) such that we have in correspondence to (28) and Fig. 9

$$p_{j+1} + x_j = x_{j+1} + \ell_{j+1}. \tag{30}$$

In order to formalize the determination of the particle energy-momentum p, we may then in "the k-process" (along $\mathcal{A}$) assume that we know the starting vertex vector x, connected to a point $\mathcal{A}_P$. We may then choose a piece k along $\mathcal{A}$ (of a size to be determined) and then define the other light-cone direction in the plane determined by (x, k) by

$$\hat{\ell} = x - k\frac{x^2}{2xk}. \tag{31}$$

The vector p will be described in terms of $(k, \hat{\ell})$ as

$$p = z\hat{\ell} + \frac{k}{2} = zx + \frac{k}{2}\left(1 - \frac{zx^2}{xk}\right), \tag{32}$$

with the requirement that the particle should be on the mass shell:

$$p^2 = m^2 = zkx \text{ i.e. } kx = \frac{m^2}{z}. \tag{33}$$

From (28) we obtain the new vertex vector x' by

$$x' = (1-z)x + \frac{k}{2}\left(1 + \frac{zx^2}{xk}\right),$$
$$(x')^2 = (1-z)(x^2 + xk) = (1-z)\left(x^2 + \frac{m^2}{z}\right). \tag{34}$$

In Fig. 10 we show both the production as described in Sect. 2 and the k-process described above. In particular we note the two areas exhibited. It is straightforward to prove that

$$A = A_r + \Gamma' - \Gamma. \tag{35}$$

with the obvious definition of e.g. $\Gamma = x^2$. The area law in (1) will be fulfilled both by the use of the area in Fig. 1 and the area in between the directrix and the hadronic curve (the X-curve) if we choose the variable z from the fragmentation function in (10) and apply it as in (32)–(34). This is so because the difference between the areas

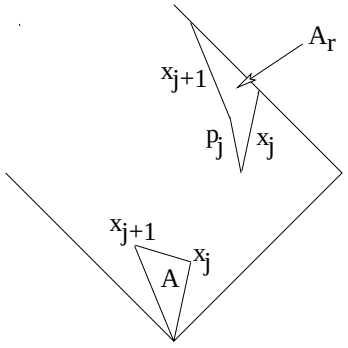

Fig. 10. The figure shows both the production as described in Sect. 2 and the k-process described in the text

A and A_r for the single step exhibited above will vanish when we consider the whole process.

It is also obvious that we may define an ℓ-process similar to the k-process we have discussed above. We just write $z\hat{\ell} = (1/2)\ell$ and introduce the variable ζ such that $(1/2)k = \zeta\hat{k}$ with ζ chosen such that $m^2/\zeta = \ell x'$. Actually we obtain the same process (although "in the opposite order") under the assumption that we start at x' and chose ℓ along the $\mathcal{B}$-part of the directrix with the variable ζ in accordance with (11). In this way the "backward" variable ζ evidently obeys the same distribution as the "forward" variable z and the area law is fulfilled.

We have reached a situation where a particle production step starts from a knowledge of a vector x connected to a light-cone direction. Then we choose a light-like vector k such that (33) is fulfilled with a z-value stochastically chosen from the fragmentation function in (10). After that we construct the particle energy-momentum and a new vector x' according to (32) and (34). We may start out choosing the "first" x-vector (x_0) equal to the q (light-cone) energy-momentum and then the $(1+1)$-dimensional model is defined.

5.2 The directrix process around a gluon corner

For a multi-gluon directrix however, we will reach situations when there are "corners", i.e. where the directrix changes direction between two colour-connected partons. Thus besides the vertex vector x, there will be a remaining light-cone vector (to the corner) c and a chosen number z such that

$$cx < \frac{m^2}{z}. \tag{36}$$

We will now consider ways to pass over such a corner. Assuming that the directrix continues on the other side of the corner we may choose a light-cone vector k which fulfils (33) (we note that according to (36) k cannot be chosen along c) and another light-cone vector c' such that

$$k + c' = c + \hat{Q} \equiv Q, \tag{37}$$

with $\hat{Q}$, a vector pointing from the corner to a new point on the directrix, and Q describing that point from the

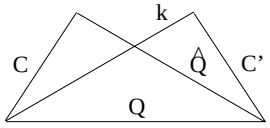

Fig. 11. A possible construction (C2) for passing a gluon corner. The figure shows the space parts of the vectors, in the rest frame of the vertex vector x, as described in the text

point on the directrix where the vertex vector x is connected.

We note that with this definition the suggested way to pass the corner corresponds to an exchange of one "dipole", $c + \hat{Q}$ in the process for another $k + c'$, i.e. to make a detour onto a "new" directrix which is "close" to the original one. The choice of the new dipole corresponds to a definition of what we will mean by the allowed "minor deviations" of the original perturbative state.

In order to investigate what can be allowed under these conditions we will exhibit a few possible choices to fulfil (37). We will then find that all possible choices are not allowed if we would like to obtain reasonable results for the final state hadron distributions. A first set of possibilities is to choose c' as a new light-like connector that will bring us "closer" (than the vector c) to the original directrix in the next production step. One may then hope that after another step in the process the new connector becomes even "smaller" so that we are back at the original directrix after a few steps.

[C1] The vector k can be chosen in the plane spanned by the vertex vector x and the directrix Q (then both c' and k are fully determined).

[C2] A more general choice is to take the vector k in the three-space spanned by x, Q and the remainder vector c. In this case it is necessary to provide a second condition to determine k and c'. In the rest frame of the vertex vector x the space parts of the vectors $\boldsymbol{c}$ and $\hat{\boldsymbol{Q}}$ span a triangle with the vector $\boldsymbol{Q}$ as baseline, cf. Fig. 11. (For the case exhibited we assume that also $\hat{Q}$ is light-like. The situation can be easily generalized to the situation when there are one or more "corners" also on $\hat{Q}$.) The remaining degree of freedom will then be fixed by an angular condition. One such condition is indicated in Fig. 11. The two triangles $(\boldsymbol{c}, \hat{\boldsymbol{Q}}, \boldsymbol{Q})$ and $(\boldsymbol{c'}, \boldsymbol{k}, \boldsymbol{Q})$ in this construction are chosen congruent. This is a kind of minimal choice for the size of Q in this three-space. It is not difficult to see that in general the new connector will be smoothly connected to the original directrix.

For the case defined by the condition C1 we obtain that k and c' will be directed along the two light-cone directions in the plane spanned by (x, Q):

$$k = \frac{Q}{2} + \frac{((Qx)Q - Q^2 x)}{2\sqrt{(Qx)^2 - Q^2 x^2}} \text{ and } c' = Q - k. \quad (38)$$

(In Fig. 11 they would be directed along the $\boldsymbol{Q}$-direction with the lengths $(Q_0 \pm |\boldsymbol{Q}|)/2$, respectively.) The vector Q contains one degree of freedom which can be fixed by multiplying with x in (38), and using (33).

This means on the one hand that the situation corresponds to using up the smallest possible segment of the directrix in the construction according to (37). On the other hand we will obtain a very sharp "bend" on the new directrix segment, defined by the dipole (kc'). While the first result is desirable from an economy point of view, the second implies that we will break the coherence conditions for the directrix (the angular ordering) as discussed in Sect. 3.1.

The fragmentation distributions obtained with this choice are not very encouraging. After we "pass" the gluon corner the density of hadrons is much higher than the density before the corner. *We find that even for a small gluonic excitation a break of coherence may result in the production of too many hadrons over a large rapidity range.*

One might hope that the situation may be mended by a suitable angular choice. This is so for the situation described in C2 for a large part of the events and for simple gluonic configurations. In Fig. 18 we show a Monte Carlo simulation of the (inclusive) final state hadron rapidities in a state containing a single gluon placed at the center with a transverse momentum of 15 GeV. Even though for most fragmentation events the choice C2 performs well, on the level of a few percent it does happen that the directions of the connecting c' and the new vertex x' are such that we obtain a situation close to the one for C1. The new directrix (possibly after a few further steps in the process) will all the time come closer to the original one; but at the same time we obtain a sharp bend farther and farther away from the original gluon corner with each step. This causes too many particles to be produced over a large rapidity range (cf. Fig. 18).

It is possible to make further changes in the procedure with more sophisticated angular choices, but we will instead go over to another and more successful choice, which we will call C3.

[C3] A natural choice for the vector c' is to make it into the k-vector for the next particle production in the process, i.e. choose a new stochastic value z' and put $c' = k'$ with

$$k'x' = \frac{m^{2\prime}}{z}, \quad (39)$$

in terms of the new vertex vector x' determined from (z, k, x) according to (34). In this way we are evidently getting back to the original directrix as fast as possible.

We may define the vector k still in the space spanned by (c, x, Q):

$$k = \alpha c + \beta x + \gamma Q. \quad (40)$$

We obtain a solution for the coefficients (α, β, γ) from the requirements

$$k^2 = 0, \quad kx = \frac{m^2}{z} \text{ and } kQ = \frac{1}{2}Q^2 \quad (41)$$

(these conditions also imply that k' is light-like), and an equation for the vector Q along the directrix using (41)

and

$$\frac{m^2}{z'} = k'x' = (Q-k)\left((1-z)x + \frac{k}{2}\left(1+\frac{zx^2}{kx}\right)\right). \quad (42)$$

In the fragmentation distribution there is a factor $(1-z)^a$ (stemming from the density of states according to the discussion around (10)). This implies that we may not use up all the energy-momentum along one of the light-cone directions in a single step. Small values of z correspond to $\zeta \simeq 1$ according to (11), i.e. to using up almost all the energy-momentum along the other light-cone direction in a step. Such values are suppressed by the area exponential in the distribution. Nevertheless it may happen that we obtain a very small z-value ($z \leq 0.1$), corresponding to a large (but not infinitely large) area. Sometimes for the general multi-gluon directrix however, there might be no possibility to accomodate such a large area due to energy-momentum conservation. Then the choice C3 cannot be done. Instead of introducing a general projection of the two-particle distributions for all such cases, in the Monte Carlo simulation we have chosen to go back to the beginning and start a new fragmentation event. Such situations, when we cannot use the choice C3, are infrequent enough to let this "restart strategy" be usable.

In order to test the influence of this feature on the model we investigate the influence on the single particle and two-particle distributions below in Sect. 6 and we find them negligible. In order to show that our changes in the directrices actually are of the hadronic mass scale we have defined a local "bending parameter" closely related to the $k_\perp$ variable used in the ordering of the Lund dipole model, cf. (50)

$$k_{\perp 2}^2 = \frac{2(xk_1)(k_1k_2)}{x(k_1+k_2)+k_1k_2}. \quad (43)$$

From the results in Sect. 6 we conclude that we are at most making local modifications on the order or below the hadronic scale in our directrices.

5.3 A differential process and its relationship to the generalized rapidity

There is a direct connection between a differential version of our hadronization process and the $\mathcal{X}$-curve that was referred to in the introduction [2]. In order to investigate this process we consider the limiting situation for a vanishing mass parameter. Then the distribution function will obviously develop a pole for $z \to 0$. We will assume that the model is defined by the incremental step size $\mathrm{d}z$ with the ratio $m/\mathrm{d}z \to m_0$. The corresponding incremental k-vector will be called $\mathrm{d}\mathcal{A}$ and it will fulfil the mass-shell condition (we will use the notation q_P instead of x for the vertex vector in connection with the differential process)

$$q_P \mathrm{d}\mathcal{A} = \frac{m^2}{\mathrm{d}z} \to \mathrm{d}z m_0^2. \quad (44)$$

From the model formulae for the change in q_P and the particle energy-momentum p ((32) and (34)) we obtain the following differential equations defining a curve to be called the $\mathcal{P}$-curve:

$$\begin{aligned} \mathrm{d}\mathcal{P} &= \mathrm{d}z q_P + \frac{\mathrm{d}\mathcal{A}}{2}\left(1-\frac{q_P^2}{m_0^2}\right), \\ \mathrm{d}q_P &= -\mathrm{d}z q_P + \frac{\mathrm{d}\mathcal{A}}{2}\left(1+\frac{q_P^2}{m_0^2}\right). \end{aligned} \quad (45)$$

Firstly we note that from the sum and differences of (45) we obtain

$$\begin{aligned} \mathcal{P} + q_P &= \mathcal{A}, \\ \mathcal{P} - q_P &= \mathcal{L}, \end{aligned} \quad (46)$$

where the vector $\mathcal{L}$ has a light-like tangent just as the directrix $\mathcal{A}$:

$$\mathrm{d}\mathcal{L} = 2\mathrm{d}z q_P - \mathrm{d}\mathcal{A}\frac{q_P^2}{m_0^2}. \quad (47)$$

In this way the $\mathcal{P}$-curve goes in between two curves with everywhere light-like tangents and the vector q_P connects to both of them.

The vector q_P is time-like and quickly approaches the length m_0. To see this we multiply the second line of (45) by q_P and obtain

$$\mathrm{d}q_P^2 = \mathrm{d}z(-q_P^2 + m_0^2). \quad (48)$$

This means (remembering that $\mathrm{d}z = q_P \mathrm{d}\mathcal{A}/m_0^2$) that we may write

$$q_P^2 = m_0^2(1-T_P^{-1}), \text{ with } T_P = \exp\left(\int\left(\frac{q_P \mathrm{d}\mathcal{A}}{m_0^2}\right)\right). \quad (49)$$

We have assumed that $q_P = 0$ and $T_P = 1$ at the start of the process. We note that the integrand in the exponent for T_P is an area, more precisely the area between the directrix and the $\mathcal{P}$-curve. This is very similar to the results we obtained in [2] for the generalized rapidity and we will now briefly connect to these results.

5.4 The $\mathcal{X}$-curve and its properties

The distribution in (1) contains two terms, the phase space and the exponential area suppression. In order to obtain a large probability it is necessary for a given total energy-momentum on the one hand to make many particles, on the other hand to make them in such a way that the area is small. The obvious compromise is that the decay region is around a typical hyperbola with an average squared distance to the origin $\langle \Gamma \rangle \equiv \Gamma_0$. The length of the hyperbola is proportional to the available rapidity range for the final state particles, i.e. $\Delta y = \ln(s/\Gamma_0)$ with s the squared c.m.s. energy.

In the Lund model interpretation for a string with a single gluon excitation, there will be two parts of the string; one spanned between the q and the g and one between the g and the $\bar{q}$. Each of them should break up

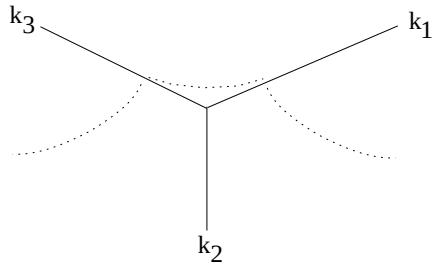

Fig. 12. A string with a $q(k_1)$, $\bar{q}(k_3)$ and a single gluon excitation (k_2). The figure shows the connected region around the gluon "tip"

in a similar way as the single string region described by (1). Besides that there will be a few particles produced in the connected region around the gluon "tip", cf. Fig. 12. If the energy-momenta of the partons are k_j, $j = 1, 2, 3$ (with indices 1 (3) for the q ($\bar{q}$)), then there will be two hyperbolic angular ranges, $(\Delta y)_{12}$ and $(\Delta y)_{23}$. The sum of these ranges is

$$\lambda = (\Delta y)_{12} + (\Delta y)_{23} = \ln\left(\frac{s_{12}}{2\Gamma_0}\right) + \ln\left(\frac{s_{23}}{2\Gamma_0}\right), \\ = \ln\left(\frac{s}{\Gamma_0}\right) + \ln\left(\frac{s_{12}s_{23}}{4\Gamma_0 s}\right). \quad (50)$$

Here $s_{j\ell} = (k_j + k_\ell)^2$ and $s = s_{12} + s_{23} + s_{13}$ and the factors 2 are introduced because only half of the gluon energy-momentum goes into each string region.

The quantity $k_\perp^2 \equiv s_{12}s_{23}/s$ is a convenient (and Lorentz invariant) approximation for the transverse momentum of the emitted gluon. From (50) we conclude that after the emission of a single gluon the phase space is increased from the single hyperbola result above by an amount corresponding to a "sticking-out tip" of length given by the logarithm of the emitted transverse momentum. In conventional notions this corresponds to the "anomalous dimensions" of QCD, i.e. the emission of a gluon increases the region of colour flow inside which more gluons can be emitted and hadronization can take place. The whole scenario is easily visualized and used in the Lund dipole model [8] and the corresponding Monte Carlo simulation program ARIADNE [9].

It is straightforward to see that if there are many gluons then there is a corresponding quantity, a generalized rapidity $\lambda \simeq \ln(\prod s_{jj+1})$ stemming from the hyperbolae spanned between the colour-connected gluons. But we note that this is not an infrared stable definition. We will now provide a convenient generalization.

A closer examination of the region around the tip of a gluon reveals that there is a correction corresponding to a connected hyperbola in the region (k_1, k_3) between the "endpoint" of the hyperbola in the region spanned between $(k_1, k_2/2)$ and the one spanned between $(k_2/2, k_3)$, cf. Fig. 12. In formulae we obtain for the average hyperbolae

$$\left(\alpha_1 k_1 + \frac{1}{2}\beta_1 k_2\right)^2 = \Gamma_0 \quad \text{and} \quad \left(\gamma_3 k_3 + \frac{1}{2}\beta_3 k_2\right)^2 = \Gamma_0,$$

$$\left(\alpha_2 k_1 + \gamma_2 k_3 + \frac{1}{2}k_2\right)^2 = \Gamma_0, \quad (51)$$

with the ranges $1 \geq \alpha_1 \geq 2\Gamma_0/s_{12}$, $2\Gamma_0/s_{12} \geq \alpha_2 \geq 0$, $2\Gamma_0/s_{12} \leq \beta_1 \leq 1$ and similarly for the other variables. The length of the two hyperbolae in the segments $(k_1, k_2/2)$ and $(k_2/2, k_3)$ are then given by (50) but the third hyperbola provides an extra contribution (in the appropriate limit $s_{13} \simeq s$) equal to $\ln(1+4\Gamma_0 s/s_{12}s_{23})$. Then the total (generalized) rapidity length becomes

$$\lambda_{123} = \ln\left(\frac{s}{\Gamma_0} + \frac{s_{12}s_{23}}{(2\Gamma_0)^2}\right). \quad (52)$$

This is evidently a nice interpolation between the situations with and without a gluon on the string and it is also an infrared stable definition of the notion of rapidity length. Equation (52) is noted in [2] and led us to introduce a functional defined on a multi-gluon string directrix.

We may firstly define a set of connected integrals [2]:

$$I_n = \int \mathrm{d}s_{01}\mathrm{d}s_{12}\cdots\mathrm{d}s_{nE}, \quad (53)$$

with the easily understood notation (cf. (18)) $s_{jj+1} = (\mathcal{A}(\xi_j) - \mathcal{A}(\xi_{j+1}))^2$, i.e. it is proportional to the squared mass between the points ξ_j and ξ_{j+1} along the directrix. By performing the integrals, we obtain that the argument in the logarithm in (52) is given by the sum $I_1/\Gamma_0 + I_2/(2\Gamma_0)^2$ and that we may in general define the functional T by

$$T = 1 + \sum_{n=1}^{\infty} \frac{I_n}{(2m_0^2)^n}, \quad (54)$$

as a suitable generalization for any string state. For a finite number of partons N the terms with $n > N$ will all vanish and we also note that the highest degree term will always have the generic form

$$2\frac{s_{12}}{4m_0^2}\frac{s_{23}}{4m_0^2}\cdots\frac{s_{N-1N}}{4m_0^2}. \quad (55)$$

We also note that for a finite total energy E the contributions for very large degrees will become smaller and smaller compared to the scale m_0.

In order to study the functional T it is suitable to introduce a varying value ξ instead of the total energy E in the connected integrals. It is then evident that the functional $T(\xi)$ will fulfil the integral equation

$$T(\xi) = 1 + \int_0^\xi \frac{\mathrm{d}s(\xi, \xi')}{2m_0^2} T(\xi'). \quad (56)$$

We will also introduce the vector-valued function $q_T(\xi)$ together with T so that we have

$$q_{T\mu}(\xi) = \frac{\int_0^\xi \mathrm{d}\mathcal{A}_\mu(\xi')T(\xi')}{T(\xi)}, \\ T(\xi) = 1 + \int_0^\xi \frac{q_T(\xi')\mathrm{d}\mathcal{A}(\xi')}{m_0^2} T(\xi'). \quad (57)$$

By differentiation and integration we obtain the results

$$T = \exp\left(\int_0^\xi \frac{q_T(\xi')\mathrm{d}\mathcal{A}(\xi')}{m_0^2}\right) \equiv \exp(\lambda(\xi)),$$
$$q_T^2(\xi) = m_0^2(1 - T^{-2}(\xi)). \qquad (58)$$

The generalized rapidity λ corresponds to the result in (52) for the simple case described above and it provides an infrared stable definition for any multi-gluon state. Further the vector q_T is time-like and will quickly approach the finite length m_0.

5.5 The correspondence between the $\mathcal{X}$-curve and the $\mathcal{P}$-curve

The similarity between these results and the results obtained for the $\mathcal{P}$-curve in (48) and (49) are obvious (besides the power in T^{-1}) and there is a correspondence to (45) and (46) also. The interpretation of the $\mathcal{X}$-curve (as worked out in [2], cf. also [3]) is that there is a vector valued function $\mathcal{X}_\mu(\lambda)$ conveniently labelled by λ such that

$$\mathcal{X} + q_T = \mathcal{A},$$
$$\frac{\mathrm{d}\mathcal{X}}{\mathrm{d}\lambda} = q_T,$$
$$\frac{\mathrm{d}q_T}{\mathrm{d}\lambda} = -q_T + \frac{\mathrm{d}\mathcal{A}}{\mathrm{d}\lambda}, \qquad (59)$$

i.e. the vector q_T is the tangent to the curve defined by $\mathcal{X}$ such that it reaches to the directrix. There is no direct correspondence to the $\mathcal{L}$-curve (unless the vectors q has reached its asymptotic length m_0).

It is useful to calculate the results from the differential equations for the case when there is a finite length light-like vector k_j in the directrix. By direct integration we find that if we have the vector q_{Tj} then "after" application of the parton energy-momentum k_j we obtain the vector q_{Tj+1} and will take a step along the $\mathcal{X}$-curve equal to $\delta\mathcal{X}_j$

$$q_{Tj+1} = \gamma_j q_{Tj} + \frac{(1+\gamma_j)}{2}k_j,$$
$$\delta\mathcal{X}_j = \left(q_{Tj} + \frac{1}{2}k_j\right)(1-\gamma_j),$$
$$\gamma_j = \frac{1}{1 + \dfrac{q_{Tj}k_j}{m_0^2}}. \qquad (60)$$

(we also note that the products of the γ_j is equal to T^{-1}). The formulae corresponding to these results for the $\mathcal{P}$-curve are

$$q'_P = \gamma q_P + \frac{\left(1 + \dfrac{q_P^2\gamma}{m_0^2}\right)}{2}k,$$
$$\delta\mathcal{P} = (1-\gamma)q_P + \frac{\left(1 - \dfrac{q_P^2\gamma}{m_0^2}\right)}{2}k,$$

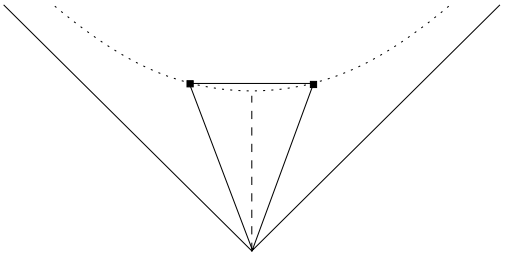

Fig. 13. Two vertices placed symmetrically (around the rapidity $y = 0$) at $m_0(\cosh(\delta y/2), \sinh(\delta y/2))$ and $m_0(\cosh(\delta y/2), -\sinh(\delta y/2))$ respectively, with a distance $2m_0\sinh(\delta y/2)$

$$\delta\mathcal{L} \equiv \ell = 2(1-\gamma)q_P - \frac{q_P^2\gamma}{m_0^2}k,$$
$$\gamma = \frac{1}{1 + \dfrac{q_P k}{m_0^2}},$$

and

$$(T_P)^{-1} = \prod \gamma_j. \qquad (61)$$

This means that while the length of a step along the $\mathcal{X}$-curve depends upon q_T^2 the corresponding step length along the $\mathcal{P}$-curve is

$$(\delta\mathcal{P})^2 \equiv M_j^2 = \frac{(1-\gamma_j)^2 m_0^2}{\gamma_j}. \qquad (62)$$

This has a very simple meaning for a step length M_j along a hyperbola with the parameter m_0, cf. Fig. 13. If the vertices are placed symmetrically around the rapidity $y = 0$ at the positions $m_0(\cosh(\delta y/2), \pm\sinh(\delta y/2))$ then the step length is evidently $2m_0\sinh(\delta y/2)$ which should be compared to M_j. Then if we square them and define $\gamma_j \equiv (1 - z_j) = \exp(-\delta y)$ the relationship in (62) will ensue.

The identification of γ and $(1 - z)$ is actually a very general feature of the process (we will come back to this aspect in the future). At this point we only note that if the lengths (proper times) of the two adjacent vertices are equal $\Gamma = \Gamma' = m_0^2 \equiv \langle\Gamma\rangle$, then from (7) we obtain

$$m_0^2 = \frac{(1-z)m^2}{z^2}, \qquad (63)$$

which evidently coincides with the result in (62). Therefore, for this particular value of z, the fragmentation process will all the time proceed along the connected hyperbolae. It is in this way that the $\mathcal{P}$-curve can be considered the average of the hadronic X-curve.

In order to provide a precise relationship between the vectors q_P and q_T as well as the functionals T_P and T we make use of an interesting relationship for the $\mathcal{X}$-curve which is derived in [2]. If we define the $(1+4)$-dimensional vector $(Q_\mu \equiv Tq_{T\mu}/m_0, T)$ (which has a length in the $(1+4)$-dimensional Minkowski metric equal to $Q^2 - T^2 =$

-1) then the differential equation for q_T can be rewritten as

$$\mathrm{d}T = Q\mathrm{d}\mathcal{A} \text{ and } \mathrm{d}Q = T\mathrm{d}A, \tag{64}$$

i.e. as a group of special rotations in this space (corresponding to a subgroup of SO(1,4)) which are defined by the incremental changes along the directrix curve. The corresponding relationship for the $\mathcal{P}$-curve is, from (44) and (45),

$$\mathrm{d}(q_P T_P) = \mathrm{d}\mathcal{A}\left(T_P - \frac{1}{2}\right) \text{ and } \mathrm{d}T_P = q_P \mathrm{d}\mathcal{A} T_P, \tag{65}$$

so that the $(1+4)$-dimensional vector $(2q_P T_P, 2T_P - 1)$ has both the same length and fulfils the same differential equations with respect to incremental changes along the directrix as (Q, T). In [2] we characterized the different directrices by means of the eigenvalues of the transfer matrix along the directrix and we found a simple and useful method to relate them to the generalized rapidity $\lambda = \ln(T)$. We will come back to this formalism in a future publication and show the significance of the extended space.

In conclusion we have found a differential version of our stochastic process which corresponds to a curve of connected hyperbolae along the directrix function. The area in between the curve and the directrix (scaled by the single parameter m_0^2) has the interpretation of a generalized rapidity measure for the multi-gluon case. It is also related to a group of rotations with the incremental steps along the directrix as the generators. The curve may be interpreted as the average hadronic curve stemming from the hadronization of the given directrix.

5.6 The reverse problem, to find the directrix from the hadronic curve

We will end this section by solving the reverse problem to the hadronization process, i.e. to exhibit to what extent we can trace the directrix from a knowledge of the hadronic curve, which we will call the X-curve in accordance with the notation introduced in Sect. 5.1.

We will assume that the X-curve is defined by the hadronic energy-momenta $\{p_j\}$, ordered and laid out according to rank. (Note that this cannot be done for a real event obtained from an experiment, since in general, rank is not an observable.) We will concentrate on the production of the hadron p_j, produced between the vertex vectors x_{j-1} and x_j with the directrix segment k_j, and an appropriately distributed stochastic number z_j. According to (28), in order to construct k_j it is sufficient to know p_j and the difference vector

$$(x_j - x_{j-1}) = \epsilon_j \hat{p}_j. \tag{66}$$

It is straightforward to solve for $\hat{p}_j$ in terms of p_j and x_{j-1}

$$\hat{p}_j = \frac{(x_{j-1}p_j)p_j - p_j^2 x_{j-1}}{\sqrt{(p_j x_{j-1})^2 - p_j^2 x_{j-1}^2}}. \tag{67}$$

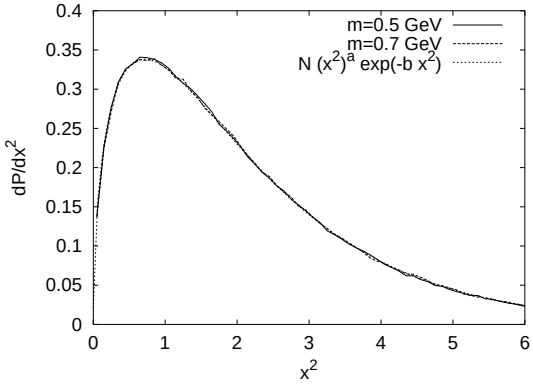

Fig. 14. The x^2 distribution of the production vertices in our method for different values of the hadron mass, together with a plot of the Γ distribution in (69) with $a = 0.5$ and $b = 0.7$

The sign ϵ_j should be positive or negative depending upon whether m^2/z_j is larger or smaller than $z_j x_{j-1}^2$ (it is useful to note that $2(p_j x_{j-1}) = (m^2/z_j + z_j x_{j-1}^2)$). Therefore if we prescribe the first vertex vector x_0 (this is always chosen in our process as the original q energy-momentum vector) then the directrix vectors as well as the vertices are determined recursively up to a sign:

$$\begin{aligned} k_j &= p_j + \epsilon_j \hat{p}_j, \\ x_j &= x_{j-1} + \epsilon_j \hat{p}_j. \end{aligned} \tag{68}$$

It is evident that the other sign will determine the corresponding ℓ_j. We note however, that neither the necessary rank-ordering of the hadrons nor the colour-ordering of the directrix gluons are experimental observables. Therefore in this form the result has solely a theoretical meaning. It is also necessary to take the possible transverse fluctuations in the fragmentation process (mentioned before as stemming from tunneling) into account before any observables can be presented.

6 Results

In the previous section, we have proposed a method of fragmenting a multi-gluon string based upon the area law. It can be described as an iterative stochastic process along the directrix curve, which fulfills the area law at every step. We have discussed a few different approaches for passing a gluon corner, cf. Sect. 5.2, and from among these we have picked a preferred one. In this section we present a few basic results from this preferred solution and we also compare it with JETSET and the other approaches we have discussed.

We start with comparing the distribution of x^2 from our model with the distribution of the proper time of the break-up points derived in the $(1+1)$-dimensional model [3]. We have

$$H(\Gamma) = N\Gamma^a \exp(-b\Gamma). \tag{69}$$

The result is presented in Fig. 14. As mentioned in the discussion at the end of Sect. 5.2, sometimes certain values of z cannot be accomodated when we pass the corner

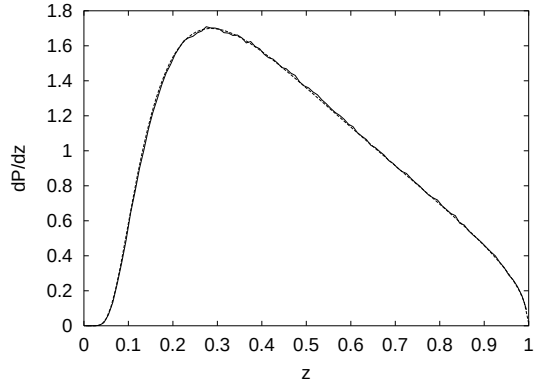

Fig. 15. z values used in particle production in our method (solid line) compared to the Lund fragmentation function $f(z)$ (dotted line). Though z value generation is according to the distribution $f(z)$, not every value produced is used. This plot shows however, that the rejection of z values in the present method is unbiased

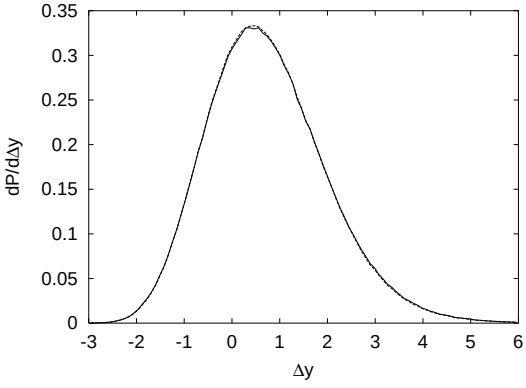

Fig. 16. The Δy distribution, defined in (70), from our method (solid line) compared with the distribution obtained using only the Lund symmetric fragmentation function (dashed line)

according to choice C3. Our Monte Carlo simulation program handles this by starting a new event from the beginning whenever this occurs. One may then expect that this might cause changes in the z distribution and also in the Γ distribution that we obtain. This is, however, not the case as can be seen from Figs. 14 and 15. Further these distributions are as they should be according to the Lund model formulae. The Γ distribution is completely independent of the mass value used just as in the standard, $1+1$-dimensional Lund model.

To examine further effects in connection with our "restart strategy", we define the following measure Δy, of the correlation between two adjacent particles in the production process

$$\Delta y = \ln\left(\frac{z_1}{z_2(1-z_1)}\right). \tag{70}$$

It corresponds to the difference in rapidity between the particles in the $(1+1)$-dimensional model. This distribution would be altered if we rejected particular correlations between successive values of z (e.g. a large value followed by a small value etc.) more often than others.

In Fig. 16 we compare our result with the result one obtains using only the Lund symmetric fragmentation function. There is no noticeable difference between the two curves, suggesting that the restart procedure (involving possible rejection of some z values) is effectively insensitive to such correlations between adjacent values.

In Fig. 17 we show the distribution of our "local bending" parameter, $k^2_{\perp 2}$, defined in (43). This figure illustrates that the modifications of the directrix that we make when we apply our method are of the order of the hadronic mass scale. For values of $k^2_{\perp 2} > m^2$ there is a fall off faster than a gaussian.

In the left-hand side plot of Fig. 18 we summarize the rapidity distributions obtained using the different approaches for passing a gluon corner, C2 and C3 described in Sect. 5.2, and compare them to a curve produced using PYTHIA in one simple situation: a perturbative string state consisting of a quark, an antiquark and a single gluon. We conclude that modifying the directrix leads to the production of too many particles over a large range of rapidity if the modifications are not "smooth". In the right-hand side of Fig. 18 we show a few rapidity distributions obtained from using our preferred method for different energies of the gluon.

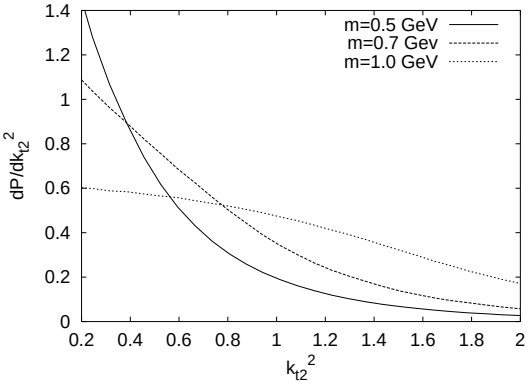

Fig. 17. Plot of $\mathrm{d}P/\mathrm{d}(k^2_{\perp 2})$ versus $k^2_{\perp 2}$ measured in $(\mathrm{GeV})^2$. Modifications of the directrix are on the scale of hadronic mass

In Fig. 19 we show an example of inclusive rapidity distributions obtained by JETSET/PYTHIA and our method. For the comparison we have used an arbitrarily chosen partonic event taken from ARIADNE. A close examination will show that in general there is a small multiplicity difference in the gluon jets. We have traced this to the fact that the two to three particles with the largest energy-momenta in the jets are faster according to our method compared to JETSET. It is impossible to compare to experimental data because firstly in this case we have only made use of a single partonic event. And secondly, at present we have not introduced the "fragmentation transverse momenta". Nevertheless we conclude that the inclusive distributions are very similar.

But we are definitely not dealing with the same particles on an event to event basis. To show this, we compare the two procedures on an exclusive, event to event basis in Fig. 20. For this plot we devised a procedure to use exactly

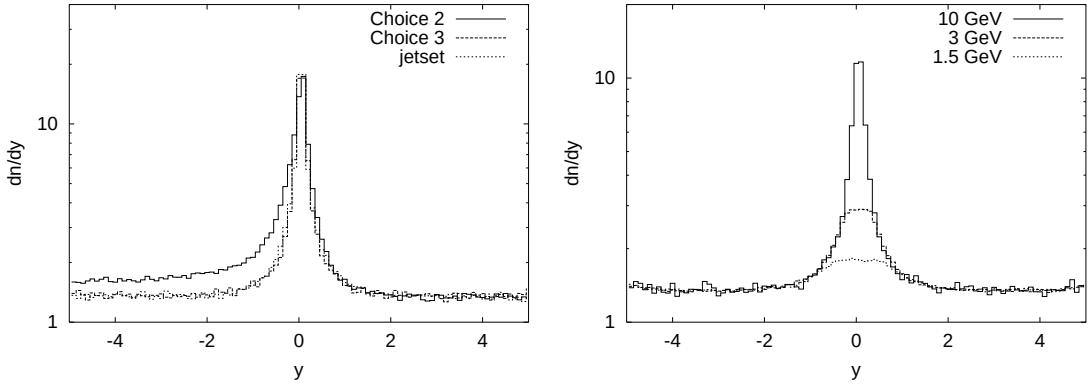

Fig. 18. The figure to the left shows rapidity distributions for different choices for the vector k. The figure to the right shows rapidity distributions for a three-jet event, obtained with the preferred method (C3), for different gluon energies. Note that the y-axis is plotted on a log scale here

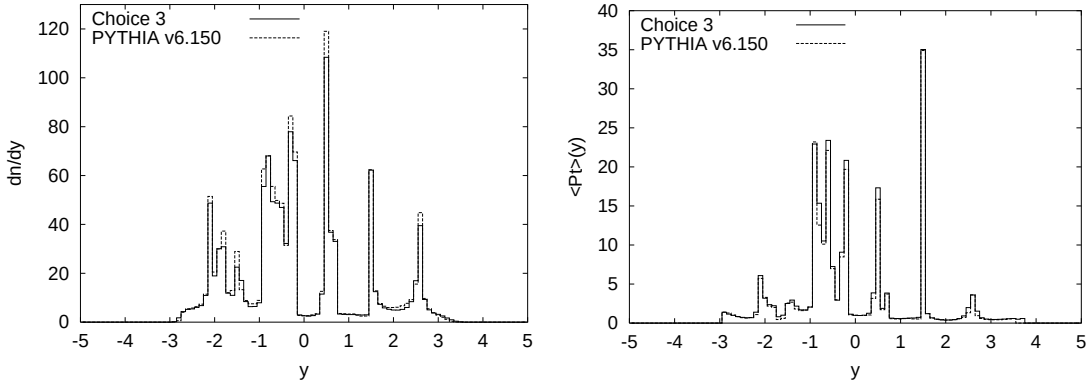

Fig. 19. The rapidity distribution (left) and mean $|p_\perp^{\rm hadrons}|$ (GeV) as a function of rapidity (right), for a string state of λ measure 70 (which is above the average λ for the energy and $p_\perp^{\rm cut}$ used for this plot: $s^{1/2} = 2000\,\mathrm{GeV}$, $p_\perp^{\rm cut} = 2\,\mathrm{GeV}$) generated by ARIADNE, fragmented using our method (solid curve) and PYTHIA (dashed curve)

the same values of z for particle production in the two programs. Since both our procedure and PYTHIA might need to reject some sequences from time to time, we took only those events where no such rejection was required by either program. We have plotted the distribution of the absolute value of the difference of the two hadronic curves, $(|\sum_{j=1}^{n}(p_{\rm C3})_j - \sum_{j=1}^{n}(p_{\rm PYTHIA})_j|^2)^{1/2}$, as a function of rank. The curve clearly shows that the hadronic curves obtained from the two programs are different. The absolute value prevents cancellation of the differences which would occur in an average over a large number of events, as we find from the comparison of the inclusive distributions.

7 Concluding remarks

We have presented a precise method to implement the Lund area law (see (1)) to fragment a multi-gluon string state. The final state hadrons are produced in an iterative stochastic process. The energy-momentum vectors $\{p_j\}$ can be laid out in rank-order as a curve, the X-curve, with a vertex vector at every point connecting to the directrix curve. The directrix corresponds to the parton energy-momentum vectors laid out in colour order. It describes on the one hand the orbit of a (massless) q-particle connected to a string and on the other hand the whole string surface.

It is possible to describe the whole process by analytical means, in particular in terms of a transfer matrix formalism similar to the one used for the $(1+1)$-dimensional model in [5]. This time it is necessary to make use of a $(1+3)$-dimensional framework. We will investigate this problem in the future.

In this paper, we have neglected the possibility of introducing transverse fluctuations in the hadronization process. Such fluctuations are introduced on the basis of tunneling arguments in the $(1+1)$-dimensional model. We feel that they are necessary for a consistent quantum mechanical treatment (there is no way to localize the string surface area better than what is allowed by Heisenberg's indeterminacy relations). We will examine the effects of such transverse fluctuations on our results in the future.

The directrix curve is in general given by a perturbative cascade (although in some cases precise matrix elements are also available). This means that the partonic states we are fragmenting are resolved only down to some cutoff, usually in virtuality or in terms of the smallest

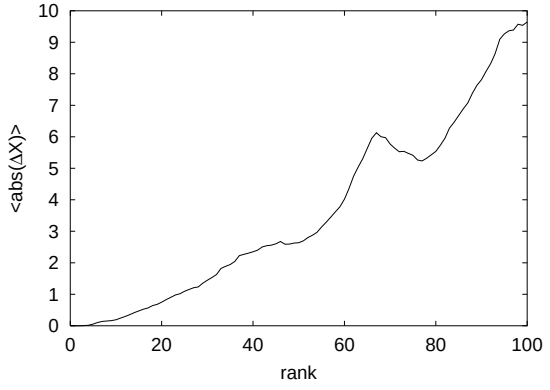

Fig. 20. Comparison of JETSET and our method on an event to event basis: We plot here the average of the absolute value of the difference (GeV) between the hadronic curves for the same partonic event used in Fig. 19, obtained from the two programs as a function of rank, where for every event the particles of a certain rank were produced using exactly the same value of z in the two alternative procedures

allowed partonic excitations. String dynamics is infrared stable in the sense that minor modifications of the directrix only have a local influence, due to the minimal nature of the string world surface. We have made use of this freedom in the fragmentation process and in this way the partonic states will be defined down to the hadronic mass scale. We will investigate the properties of the soft gluons thus introduced into the partonic state, in the future.

We have shown that the fragmentation process, with step size equal to the hadronic mass can be defined also in the limit of a vanishing mass in terms of a differential process. The corresponding solution, the $\mathcal{P}$-curve, is stretched in between two curves, the original directrix, $\mathcal{A}$, and another curve, the $\mathcal{L}$-curve, also with a light-like tangent. The correspondence to the vertex vectors for the fragmentation process are connectors to the $\mathcal{P}$-curve reaching out to the $\mathcal{A}$- and the $\mathcal{L}$-curves. The area in between the $\mathcal{P}$-curve and the directrix $\mathcal{A}$ corresponds to a generalized rapidity variable in the same way as the average hyperbola defines rapidity for the $(1+1)$-dimensional model. There is an interesting relationship to the group of rotations in a $(1+4)$-dimensional space which we will investigate further in the future.

We have also shown that there is a duality (with properties similar to the parton–hadron duality introduced by the St. Petersburg group [10]) between hadronic X-curve, defined by our process, and the original directrix. We note, however, that the hadrons produced in our process always stem from the energy-momenta of two or more partons. The vertex vectors x_j contain the "memory" of the earlier partons. It is nevertheless possible to reconstruct the directrix from the X-curve, although the relationship contains a large number of degrees of freedom (the number of degrees of freedom increases further if we introduce transverse momentum fluctuations in the fragmentation process). We will investigate these properties in the future.

The process we have defined has also been implemented into a Monte Carlo simulation program. Due to the way it is constructed it is fairly direct to include also the multi-particle production features of the original JETSET, i.e. to include probabilities for different $(q\bar{q})$-flavors, different kinds of mesons, the decay of resonances etc. This is necessary for a comparison with experimental data.

Acknowledgements. We would like to thank G. Gustafson for extensive discussions and T. Sjöstrand and L. Lönnblad for a lot of help both with the material and in particular with the way the Monte Carlo programs JETSET and ARIADNE work.

References

1. B. Andersson, G. Gustafson, B. Söderberg, Z. Phys. C **20**, 317 (1983)
2. B. Andersson, G. Gustafson, B. Söderberg, Nucl. Phys. B **264**, 29 (1986)
3. B. Andersson, The Lund model (Cambridge University Press, 1998)
4. T. Sjöstrand, Computer Phys. Commun. **82**, 74 (1994)
5. B. Andersson, F. Söderberg, Eur. Phys. J. C **16**, 30 (2000)
6. T. Sjöstrand, Nucl. Phys. B **248**, 469 (1984)
7. Ya.I. Azimov et al., Phys. Lett. B **165**, 147 (1985). Yu.L. Dokshitzer, V.A. Khoze, S.I. Troyan, in Perturbative QCD, edited by A.H. Mueller (World Scientific) p. 241
8. G. Gustafson, U. Pettersson, Nucl. Phys. B **306**, 746 (1988)
9. L. Lönnblad, Ariadne v 4.10, Computer Phys. Commun. **71**, 15 (1992)
10. Yu.L. Dokshitzer, S.I. Troyan, Proceedings of the XIX Winter School of the LNPI, **1**, 144 (1984); Ya.I. Azimov, Yu.L. Dokshitzer, V.A. Khoze, S.I. Troyan, Z. Phys. C **27**, 6 (1985)